Available online at www.sciencedirect.com
SCIENCE DIRECT®
Carbohydrate Research 340 (2005) 1335–1342
Carbohydrate RESEARCH

# Mango ripening—chemical and structural characterization of pectic and hemicellulosic polysaccharides

Hosakote M. Yashoda, Tyakal N. Prabha and Rudrapatnam N. Tharanathan*

*Department of Biochemistry and Nutrition, Central Food Technological Research Institute, Mysore 570020, India*

Received 18 August 2004; received in revised form 7 February 2005; accepted 22 March 2005
Available online 12 April 2005

**Abstract**—Ripening of mango is characterized by a gradual, but natural softening of the fruit, which is due to progressive depolymerization of pectic and hemicellulosic polysaccharides with significant loss of galactose, arabinose and mannose residues at the ripe stage. Structural characterization employing permethylation followed by GC–MS analysis, IR and $^{13}C$ NMR measurements revealed the major CWS fractions of both unripe and ripe mangoes to be of variable molecular weights and having a 1,4-linked galactan/galacturonan backbone, which is occasionally involved in side chain branches consisting of single residues of galactose and arabinose or oligomeric 1,5-linked arabinofuranose residues linked through 1,3-linkages; whereas the major hemicellulosic fractions of unripe mango to be of xyloglucan-type having 1,4-linked glucan backbone with branching by non-reducing terminal arabinose and xylose residues.


*Keywords:* Mango ripening; Polysaccharides; Structural characterization; Pectin; Galacturonan; Xyloglucan

## 1. Introduction

Much of the work in the area of fruit ripening has been focused on changes with specific reference to textural softening. The latter is mainly due to alterations in cell wall structure and composition, wherein pectin and hemicelluloses are the major contributors. It has been shown that the solubilization of pectic polymers during mango fruit ripening is much more extensive than in tomato[1] and kiwi[2] fruits. Nevertheless, the degradation of pectins in relation to textural softening differs from fruit to fruit. Many reports have focused on considerable pectin degradation that coincides with fruit softening vis-a-vis expression of polygalacturonase (PG) enzyme.[3,4] However, molecular genetic approaches have revealed that PG-dependent pectin degradation is not essential for fruit softening,[5,6] but it may play a role in other aspects of fruit quality.[7] A few recent studies have examined the extent of hemicellulose degradation during fruit ripening, and it has been demonstrated that xyloglucan undergoes substantial depolymerization in many ripening fruits.[8,9] It is very well documented that plant cell walls consist of cellulose microfibrils coated with cross-linked xyloglucans, and disruption of such a network (or matrix) may be a key element in regulating cell wall integrity. Except for gross compositional changes,[10,11] very little is known about the structural modifications in the cell wall during mango (*Mangifera indica* L., cv. Alphonso) fruit ripening. The main objective of this study was to elucidate the depolymerization changes in ripening Alphonso mango, especially with respect to alterations in composition, molecular weight and structural characteristics of a few major pectic and hemicellulosic polysaccharides.

## 2. Experimental

### 2.1. Materials

Mature green mango (*M. indica* L., cv. Alphonso) fruits were freshly harvested from orchards through a local

* Corresponding author. Tel.: +91 0821 2514876; fax: +91 0821 2517233; e-mail: tharanathan@yahoo.co.uk

0008-6215/$ - see front matter © 2005 Published by Elsevier Ltd.
doi:10.1016/j.carres.2005.03.004

dealer, washed thoroughly with running tap water, wiped with ethanol and stored at ambient temperature for normal ripening (10–12 days after harvest). The fruit pulp from unripe and ripe mango fruits was used for the isolation of various polymeric fractions, as described elsewhere.[10] All the reagents/chemicals used were of high purity standards. $Ac_2O$, pyridine and dimethyl sulfoxide were purified by vacuum distillation and the constant boiling fraction was collected.

### 2.2. Polysaccharide fractionation

The alcohol-insoluble residues from unripe and ripe mango pulp were subjected to sequential extraction with water at ambient and elevated (80 °C) temperatures, 0.5% EDTA, 0.05 M $Na_2CO_3$ containing 0.02 M $NaBH_4$ and 4 N NaOH under $N_2$ atmosphere.[10] Each time the extracted polysaccharides were precipitated by adding ethanol (3 vol), followed by dialysis of their aqueous solution and lyophilization, whereas the alkali extract was subjected to differential precipitation with 4 M acetic acid at 4 °C followed by centrifugation, and ethanol precipitation of the supernatant to get hemicelluloses A and B, respectively. The final alkali-insoluble residue was designated as cellulosic fraction as it was rich in glucose.

### 2.3. Analytical methods

Total carbohydrates and uronic acid were determined by phenol–sulfuric acid[12] and metahydroxy biphenyl methods,[13] respectively.

Crude CWS and hemicellulosic polysaccharides were purified by chromatography on DEAE–cellulose column (3.2 × 26 cm) eluted with increasing gradients of ammonium carbonate (0.05–0.45 M) and sodium hydroxide (0.05–0.45 M) solutions at a flow rate of 60 mL/h. Fractions (8 mL) were assayed for total sugars. GPC was performed on Sepharose CL-4B column (1.4 × 100 cm, 175 mL bed volume) equilibrated and eluted with 0.1 M NaCl at a flow rate of 18 mL/h. The column was pre-calibrated with T-series dextrans of known molecular weight values. A calibration curve was prepared by plotting $V_e/V_o$ (elution volume/void volume, mL) versus log molecular weight and molecular weight of the unknown polysaccharide was determined.

High performance size exclusion chromatography (HPSEC) was performed in a Shimadzu HPLC system (HIC-6A System controller, CR-4A Chromatopac integrator and LC-6A pump), fitted with E-linear and E-1000 μ-Bondapack columns (30 cm × 3 mm i.d.) connected in series with a guard column and Shimadzu RID-6A RI detector set at $8 \times 10^{-6}$ RIU. The fractions (10 mg/mL, 10 μL loaded) were individually loaded and eluted with water at a flow rate of 0.6 mL/min at 40 °C.

The polysaccharides were acid hydrolyzed either by 72% $H_2SO_4$ followed by 8% $H_2SO_4$ at 100 °C for 10 h or by 2 M TFA at 120 °C for 1 h. Alditol acetate derivatives were prepared[14] and analyzed by GC on Shimadzu GC-15A system fitted with 3% OV-225 (8 ft × 1/8″ ss column maintained at 200 °C), FID and CR4-A monitor.

### 2.4. Structural analysis

Specific rotation of the polysaccharides was determined using a Perkin–Elmer (model 243) spectropolarimeter at 20 °C. Carboxyl reduction of CWS was carried out according to Taylor and Conrad,[15] the reduction was repeated thrice to obtain a sample containing <2% GalA. Permethylation of native and carboxyl-reduced polysaccharides was carried out using dimsyl anion and $CH_3I$, according to Hakomori.[16] The permethylated alditol ($^2H$) acetates were analyzed by GC–MS on a high performance quadrupole Shimadzu QP-5000 MS coupled with GC-17A, using SP-2330 capillary column (30 m × 0.31 mm i.d., 0.02 μ coating) operating at an ionization potential of 70 eV with a temperature programme mode of 180–200 °C at 4 °C rise/min. The mass range was 40–400 amu ($m/z$) and helium was the carrier gas.

### 2.5. Spectral measurements

FT-IR spectral measurements were done in a Perkin–Elmer IR spectrometer 2000 operating at 4 $cm^{-1}$ resolution using KBr pellet. $^{13}C$ NMR spectra were recorded in Bruker AMX 400 MHz NMR spectrometer (using 5 mm multi-nucleus probe) operating at 60 °C for 4 h using a spectral width of 227 Hz with 6000 scans. The purified samples (25 mg) were dissolved in $D_2O$ (1 mL) and the deuterium resonance was used as a field frequency lock and the chemical shifts were referenced to external TMS.

## 3. Results and discussion

### 3.1. Pectic polysaccharides

The various polysaccharide fractions from unripe and ripe mangoes were extracted sequentially on the basis of their differential solubility, as reported earlier.[10] The yield and sugar composition of the isolated polysaccharide fractions are given in Table 1. The content of water-soluble polysaccharide (CWS) of ripe mango (0.615 g %, FW) was ~20% less in comparison with that of unripe mango (0.755 g %, FW). Whereas, on the basis of total cell wall polysaccharides, the percent yield of CWS from ripe mango was twice (26.8%) that of unripe mango (12.7%, see Table 1), which may be attributed to better

**Table 1.** Yield and sugar composition of the polysaccharide fractions of mango

| Fractions | Yield | | | | Sugar composition (mg %)[a] | | | | | | | | | | | | GalA | |
|---|---|---|---|---|---|---|---|---|---|---|---|---|---|---|---|---|---|---|
| | g/100 g FW | | % Cell wall polysaccharides | | Rha | | Ara | | Xyl | | Man | | Gal | | Glc | | | |
| | A | B | A | B | A | B | A | B | A | B | A | B | A | B | A | B | A | B |
| Cold water solubles | 0.76 | 0.62 | 12.7 | 26.8 | 0.2 | 0.1 | 1.6 | 0.7 | 0.1 | 0.2 | 1.2 | 0.1 | 1.9 | 0.6 | 55.7 | 2.5 | 14.3 | 21.5 |
| Hot water solubles | 0.55 | 0.31 | 9.2 | 13.4 | 0.4 | 0.1 | 2.3 | 4.3 | 0.04 | 2.0 | 0.1 | 0.5 | 1.7 | 2.8 | 15.3 | 21.7 | 11.9 | 21.5 |
| Pectic fractions | 1.86 | 0.38 | 31.1 | 16.5 | 0.4 | 0.3 | 2.5 | 1.4 | 1.4 | 0.1 | 0.3 | 0.1 | 1.4 | 0.5 | 36.4 | 3.3 | 12.2 | 18.9 |
| Hemicelluloses | 0.80 | 0.20 | 13.4 | 8.7 | 0.3 | 0.8 | 2.0 | 4.2 | 2.2 | 12.7 | 0.8 | 1.8 | 0.8 | 4.8 | 77.9 | 60.0 | 6.1 | 9.4 |
| Cellulose | 2.03 | 0.80 | 33.9 | 34.6 | — | — | 0.4 | 0.2 | 0.4 | 0.5 | 0.4 | 0.8 | 0.8 | 0.3 | 90.2 | 76.2 | — | — |

A, unripe mango; B, ripe mango; FW, fresh weight.
[a] By GC, as alditol acetates.

solubilization of some of the polysaccharide fractions as a result of ripening-induced structural changes. Nevertheless, the galacturonic acid to neutral sugar ratio of CWS was higher in the ripe (0.6:1) than unripe (0.2:1) mango, indicating a more pronounced elimination of neutral sugar residues during ripening. A similar loss of acidic and neutral sugars was observed in total pectic fraction of ripening persimmon[17] and 'Ngowe' mango.[18] Loss of galacturonic acid was also reported in a few other varieties of mango.[19] Upon DEAE–cellulose ion exchange chromatography (IEC) considerable qualitative and quantitative changes were observed in the fractionation profile, viz., a significant decrease in the relative percent yield of most of the fractions was evident from unripe to ripe mango (Fig. 1). The percent yield of the major fraction II, eluted with 0.15 M $(NH_4)_2CO_3$ and fraction IV, eluted with 0.2 M $(NH_4)_2CO_3$, was decreased by about 10% and 40%, respectively, upon ripening. Nevertheless, there was no complete disappearance of any of the fractions at the end of ripening, which indicated a rather controlled depolymerization of CWS. Accordingly, the GPC and HPSEC patterns of Fr. II and Fr. IV showed a shift to lower molecular weight material upon ripening (Fig. 2). The broad molecular weight distribution of Fr. II and Fr. IV from unripe to ripe stage was 1818–1000 kDa and 1990–126 kDa, respectively. Similar observations have been made on the IEC and GPC profiles of CWS fractions of fruits, such as bush butter fruit,[20] tomato[21] and peach.[22]

Being the major fraction, CWS Fr. II from unripe and ripe mangoes was further studied for any ripening-induced structural changes. The purified Fr. II showed mainly galactose and arabinose with almost a comparable pentose to hexose ratio and galacturonic acid content (24%) (see Table 2). The decrease from unripe to ripe stage in arabinose to galactose ratio (1:1.4 to 1:1.2, respectively) indicated degradation of arabinogalactan-type polysaccharide during ripening. The presence of rhamnose in them may possibly indicate that these polymers are pectic-derived polysaccharides,

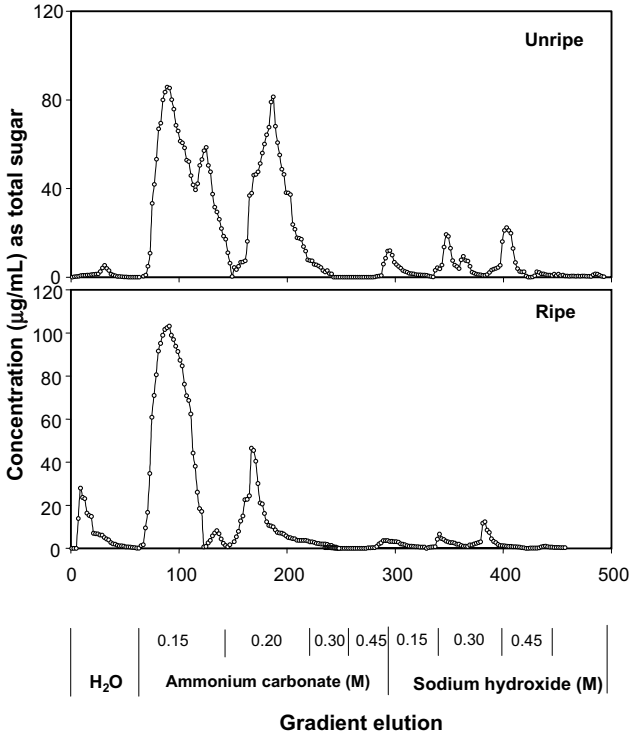


**Figure 1.** DEAE–cellulose profile of CWS polysaccharides from unripe and ripe mangoes.

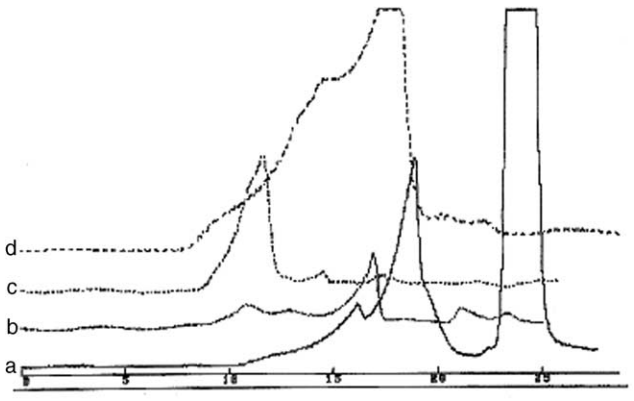


**Figure 2.** HPSEC profiles of CWS Fr. II and IV from unripe (a, b) and ripe (c, d) mangoes.

**Table 2.** Sugar composition (%) of the major CWS Fr. II of unripe and ripe mangoes

| Fr. II | Total sugars | GalA | Rha | Ara | Xyl | Gal | Glc | Ara:Gal | $[\alpha]_D^0$ [a] |
|---|---|---|---|---|---|---|---|---|---|
| Unripe mango | 82.7 | 23.6 | 3.4 | 20.9 | 1.5 | 28.9 | 3.6 | 1:1.383 | +247.4 |
| Ripe mango | 98.0 | 24.4 | 6.3 | 25.8 | 1.7 | 31.7 | 3.3 | 1:1.229 | +272.0 |

[a] In water, *c* 0.5%.

wherein the arabinogalactan side chains are linked to polygalacturonic acid main chain through rhamnose residues, as also reported for several other pectins.[23,24] A similar overall loss of galactosyl and rhamnosyl residues with concomitant increase in polydispersity during mango fruit ripening was attributed to progressive depolymerization of chelator-soluble pectic fraction.[25] A close correlation between the distribution of pectic substances and tissue softening in ripening Keitt mangoes was established.[26] The high positive specific rotation for these fractions (Table 2) indicated that the anomeric configuration of the main chain is probably of α-type. A high positive specific rotation has also been reported for purified citrus (+277°), apple (+300°) and sunflower (+308°) pectins.[27] To facilitate knowing the structural involvement of galacturonic acid moieties the fractions were carboxyl reduced (<2% uronic acid) prior to permethylation and GC–MS analysis. From the results presented in Table 3, it is obvious that Fr. II of both unripe and ripe mango is indeed a pectic-type polysaccharide having arabinogalactan side chain appendages. Identification through diagnostic mass fragments (*m*/*z*, Table 3) of 2,3,6-$Me_3$-Gal revealed a 1,4-linkage in the backbone, which could either be derived from homogalacturonan or from type I galactan. Nevertheless, the main chain was further involved in extensive branching as shown by the presence of 2,3-$Me_2$- and 2-Me-galactose derivatives, which are derived from O-6 and O-3/O-6 disubstituted monomeric residues. Possibly, both galactose and arabinose were found involved as oligomeric side chains, linked to the galactan backbone. All the rhamnose (2,3,4-$Me_3$-Rha) and a portion of arabinose (2,3,5-$Me_3$-Ara) and galactose (2,3,4,6-$Me_4$-Gal) were found to be involved at non-reducing terminal units. The arabinan side chain was essentially 1,5-linked and having O-3 monosubstituted branch-off residues of arabinose (identification of 2-Me-Ara). In the ripe mango Fr. II, the degree of branching with respect to arabinose was relatively more in comparison with that of unripe Fr. II (1 vs 3 mol of 2-Me-Ara), probably due to selective depolymerization of some of the side chain branch-off residues during ripening. Quantitative variations in other structural segments of ripe and unripe mango Fr. II were also observed, in addition to their differences in molecular size. Possibly, degradation of some of the side chains may allow loosening of the cell wall structure with improved solubilization of polysaccharides. Arabinose was found to exist in labile furanoside form, whereas galactose and galacturonic acid were in pyranosidic linkage. The relative molar ratios of arabinose (1:1.2 and 1:1.17) to galactose (1:1 and 1:1.09) before and after permethylation, as well as the ratio of terminal to branching residues (4.1:4.3 in unripe and 3.6:4.4 in ripe mango) were in good agreement, thus unambiguously supporting the structural features deduced. Arabinogalactan side chains with similar types of linkages have been reported earlier.[27]

Small amounts of glucose found in the sugar analysis (see Table 2) revealed itself upon methylation (see Table 3) in the form of 2,3,6-$Me_3$- and 2,3-$Me_2$-derivatives, which signifies its presence as a linear 1,4-linked glucan. Probably the presence of this glucan could be attributed to the possible existence of associated polysaccharides through polymer–polymer interactions. Identification

**Table 3.** *O*-Methyl ethers derived from carboxyl-reduced and permethylated CWS Fr. II from unripe and ripe mangoes

| Monosaccharide | *O*-Methyl ether | Molar ratio | | Diagnostic mass fragments (*m*/*z*) | Mode of linkage |
|---|---|---|---|---|---|
| | | Unripe | Ripe | | |
| Rha | 2,3,4-$Me_3$ | 0.4 | 1.0 | 43, 102, 118, 131, 162, 175, 206, 219 | Rha*p*-(1→ |
| Ara | 2,3,5-$Me_3$ | 3.5 | 3.2 | 43, 45, 118, 161, 162, 205 | Ara*f*-(1→ |
| | 2,3-$Me_2$ | 3.5 | 3.4 | 43, 118, 129, 162, 189, 233 | →5)-Ara*f*-(1→ |
| | 2-Me | 1.3 | 3.1 | 43, 118, 201, 261 | →3,5)-Ara*f*-(1→ |
| Gal | 2,3,4,6-$Me_4$ | 0.2 | 0.1 | 43, 45, 101, 118, 129, 161, 162, 205, 249 | Gal*p*-(1→ |
| | 2,3,6-$Me_3$ | 10.0 | 10.0 | 43, 45, 118, 131, 162, 173, 203, 233, 277 | →4)-Gal*p*-(1→ |
| | 2,3-$Me_2$ | 2.0 | 1.1 | 43, 118, 129, 162, 189, 201, 261, 305 | →4,6)-Gal*p*-(1→ |
| | 2-Me | 0.3 | 0.2 | 43, 118, 173, 261, 301, 333 | →3,4,6)-Gal*p*-(1→ |
| Glc | 2,3,6-$Me_3$ | 0.2 | 0.4 | 43, 45, 118, 131, 162, 173, 203, 233, 277 | →4)-Glc*p*-(1→ |
| | 3,4-$Me_2$ | 2.0 | 2.0 | 43, 129, 130, 189, 190, 233 | →2,6)-Glc*p*-(1→ |
| | 2,3-$Me_2$ | 1.0 | 1.0 | 43, 118, 129, 162, 233, 261, 305 | →4,6)-Glc*p*-(1→ |

of 3,4-$Me_2$-glucose derivative in here is, nevertheless surprising as it indicates rather a different type of main chain linkage. These glucopyranosyl structural units belong more to glucan oligomers.

Thus, the acidic polysaccharide fractions from unripe and ripe mangoes were essentially of pectic-type having a main chain of 1,4-linked D-galacturonic acid and 1,4-linked galactan residues with side chain appendages at several locations, of arabinose and galactose mono- and oligomers. These structural features are reminiscent of those found in several other fruit pectins.[28–30]

FT-IR spectra of the purified Fr. II (Fig. 3) showed absorptions at 3401 $cm^{-1}$ (indicative of free unsubstituted –OH groups), 1739 $cm^{-1}$ (ester bonds) and 1606 $cm^{-1}$ (due to carboxylate functional group).[31] Intense peaks at 1100 and 1015 $cm^{-1}$ corresponded to galacturonic acid residues. The absorbance at 1402 $cm^{-1}$, indicative of the presence of pectin methyl ester group (–$OCH_3$), probably suggests that some of the uronic acid carboxyls are esterified.[31] Absorption at 1238 $cm^{-1}$ indicated the presence of acetyl groups as reported before.[32] A rather weak absorbance at 835 $cm^{-1}$ was indicative of α-configuration, which also correlated with their specific rotation values. A minor absorption peak at 893 $cm^{-1}$ for both the fractions was attributed to possible β-glycosidic linkages between the neutral sugar residues in the side chain. The absorbance at 953 $cm^{-1}$ was indicative of a high content of galactose, whereas an intense peak at 1015 $cm^{-1}$ may correspond to arabinan side chain.[31]

The nature of anomeric ring carbons was further unequivocally established by $^{13}C$ NMR spectral analysis (Fig. 4), which showed signals characteristic of pectic type polysaccharides.[33–35] The spectral quality was rather poor, probably due to viscous nature of the samples at concentrations required for good NMR analysis. Furthermore, the monomeric residues occurring in the main chain of the polysaccharide are too large and may be rigid enough to yield detectable signals, as strong signals are the result of highly flexible chains.[33] The signal in the region 100.8 ppm corresponded to C-1, 71–76 ppm to C-4, C-2, C-3 and C-5 whereas that

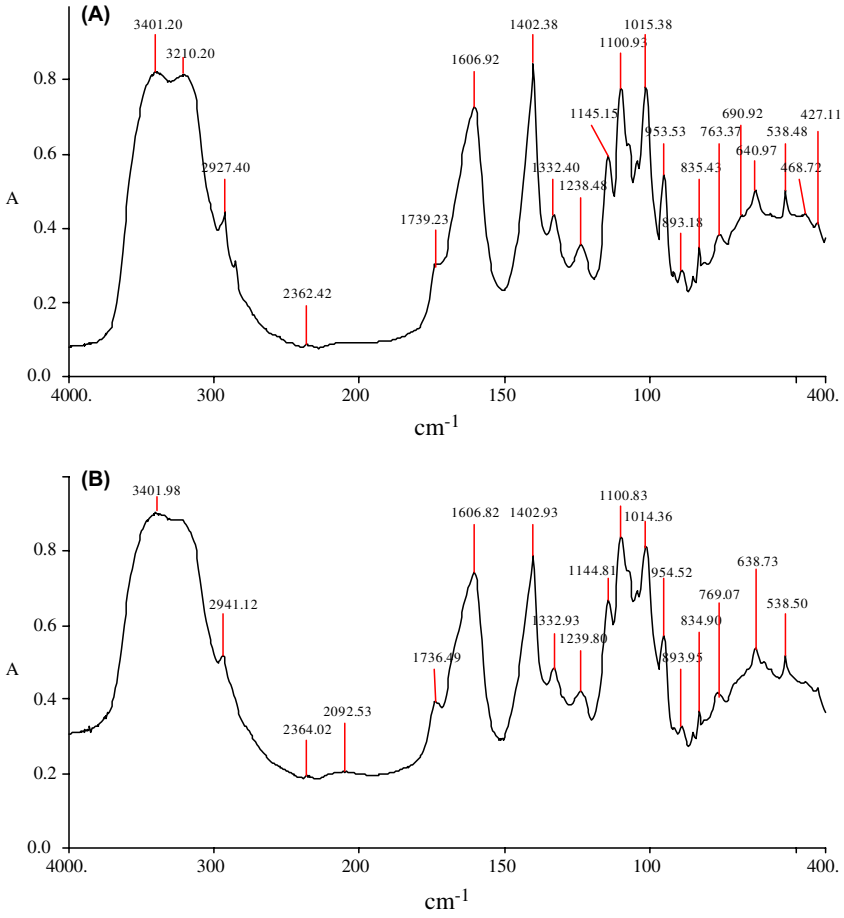


**Figure 3.** FT-IR spectra of CWS Fr. II from unripe (A) and ripe (B) mangoes.

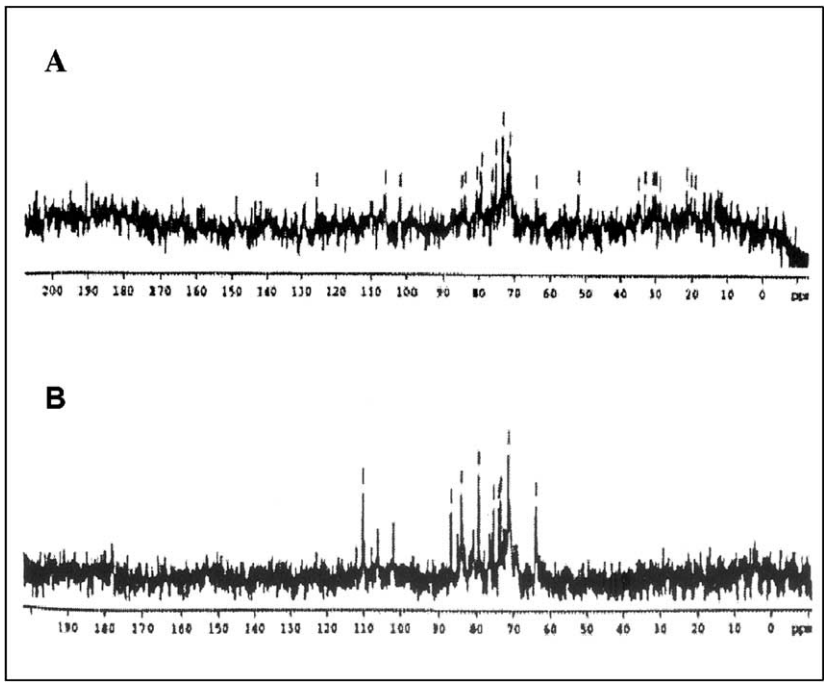


**Figure 4.** $^{13}C$ NMR spectra of CWS Fr. II from unripe (A) and ripe (B) mangoes.

at 60–62 ppm was assigned to C-6. The assigned signals showed a close similarity with those of α-galacturonan isolated from mung bean hypocotyls and flax,[30] sugar beet,[31] tomato[1] and kiwi fruit[34] pectins.

### 3.2. Hemicellulosic polysaccharides

Contribution of hemicellulosic polysaccharides towards textural softening phenomenon was observed in tomato,[9] muskmelon[35] and other fruits.[8,9] In ripening mango, a striking drop in abundance and molecular weight of the alkali-soluble hemicellulosic fractions IV and V was observed (Fig. 5, see Table 1), the decrease was over fourfold from unripe (0.795 g % FW) to ripe (0.185 g % FW) stage. The galacturonic acid to neutral sugar ratio was higher in the ripe stage than unripe stage, indicating a more pronounced dissolution of neutral sugar residues. Upon DEAE–cellulose fractionation, the hemicellulosic polysaccharides were resolved into several fractions (Fig. 6), of which fractions IV and V, eluting

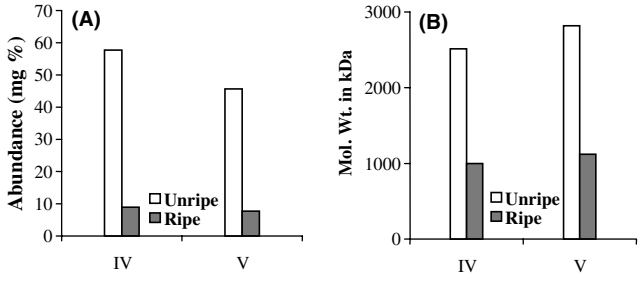


**Figure 5.** Abundance (A) and molecular weight (B) changes of the major hemicellulosic fractions from unripe and ripe mangoes.

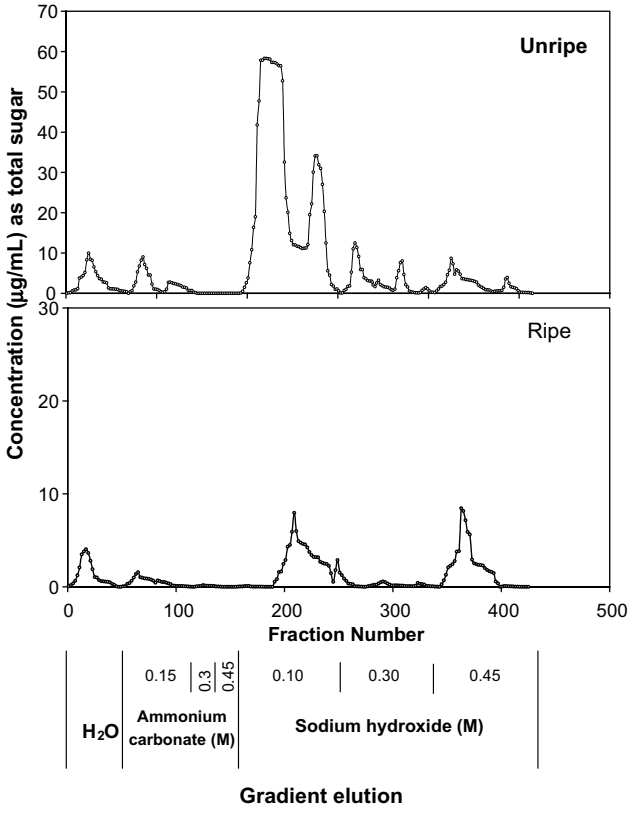


**Figure 6.** DEAE–cellulose profile of hemicellulosic polysaccharides from unripe and ripe mangoes.

with 0.10 M NaOH were the major (>80% recovery). The mg % drop in their levels from unripe to ripe stage was significant: 47.7–7.9% and 35.6–6.7%, respectively. Concomitantly, considerable drop in arabinose, xylose and glucose contents of these fractions was evidenced as a result of ripening, which correlated with their drop in molecular weight values: 2512–1000 kDa and 2818–1122 kDa, respectively, for fractions IV and V from unripe to ripe stage. The content and molecular weight of cell wall hemicellulosic fractions were found to decrease with ripening in two cultivars, viz., Keitt and Tommy Atkins of mango fruits.[19] Due to their extensive depolymerization during fruit ripening, only those hemicellulosic fractions derived from unripe mango (Fig. 7) were chosen for structural studies.

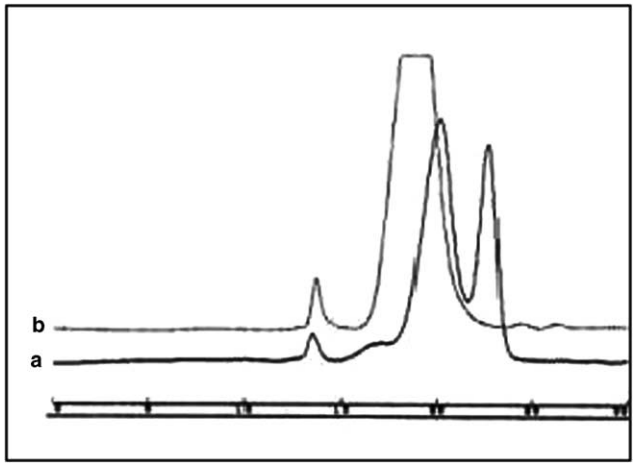


**Figure 7.** HPSEC profiles of hemicellulose Fr. IV (a) and V (b) of unripe mango.

Upon fractionation on Sepharose CL-4B they were eluted in the void volume, indicating them to be of very high molecular weight. Compositional analysis (Table 4) indicated that both the fractions are rich in glucose and xylose with smaller amounts of arabinose, mannose and rhamnose, the latter was found especially in Fr. IV, suggesting possibly a xyloglucan-type polysaccharide in them. The low Xyl:Glc ratio (1:3.8) of Fr. IV was indeed uncommon for xyloglucan, not reported before. The low positive specific rotation indicated their anomeric configuration to be of β-type. Upon permethylation analysis of Fr. IV (see Table 5) identification of structural elements [→4)-Glc*p*-(1→ and →4,6)-Glc*p*-(1→] indicated a branched 1,4-linked glucan backbone. Some of these residues were found involved in multiple branching at O-3 and O-3/O-6 as shown by the presence of 2,6-$Me_2$-glucose and glucitol derivatives, respectively. Over one third of the main chain glucosyl moieties were involved in additional branching as indicated by their relative molar ratios (Table 5). Both arabinose and xylose constituted the side chain branch-off residues, with xylosyl units being further involved in multiple branching (identification of 2-Me-Xyl*p*). Majority of arabinose and a part of xylose were found located at the non-reducing terminal ends (presence of 2,3,5-$Me_3$-Ara*f* and 2,3,4-$Me_3$-Xyl*p*). Arabinose was present in its labile furanoside form whereas xylose and glucose moieties were in pyranoside ring form.

On the other hand, permethylation data of Fr. V showed considerable variations in its overall structural

**Table 4.** Sugar composition (%) of hemicellulosic Fr. IV and V of unripe mango

| Fr. | Total sugars | GalA | Rha | Ara | Xyl | Man | Gal | Glc | Xyl:Glc | $[\alpha]_D^0$ [a] |
|---|---|---|---|---|---|---|---|---|---|---|
| IV | 98.0 | 1.6 | 2.0 | 3.6 | 17.7 | 5.3 | 1.2 | 67.5 | 1:3.81 | +64.0 |
| V | 98.0 | 1.0 | 0.4 | 5.2 | 4.9 | — | 1.4 | 64.2 | 1:13.10 | +32.0 |

[a] In water, *c* 0.5%.

**Table 5.** *O*-Methyl ethers derived from permethylated hemicellulosic Fr. IV and V of unripe mango

| Monosaccharide | *O*-Methyl ether | Molar ratio | | Diagnostic mass fragments (*m/z*) | Mode of linkage |
|---|---|---|---|---|---|
| | | Fr. IV | Fr. V | | |
| Ara | 2,3,5-$Me_3$ | 2.3 | 2.0 | 43, 45, 118, 161, 162, 205 | Ara*f*-(1→ |
| | 3,5-$Me_2$ | 1.0 | — | 43, 45, 101, 129, 130, 161, 190 | →2)-Ara*f*-(1→ |
| Xyl | 2,3,4-$Me_3$ | 1.3 | 1.2 | 101, 102, 118, 129, 145, 161, 162, 205 | Xyl*p*-(1→ |
| | 2,3-$Me_2$ | 5.0 | 3.0 | 118, 162, 189, 233 | →4)-Xyl*p*-(1→ |
| | 2-Me | 1.3 | — | 43, 118, 129, 143, 201, 261 | →3,4)-Xyl*p*-(1→ |
| Glc | 2,3,4,6-$Me_4$ | — | 1.0 | 43, 45, 101, 118, 129, 161, 162, 205, 249 | Glc*p*-(1→ |
| | 2,4,6-$Me_3$ | — | 1.3 | 43, 45, 101, 118, 129, 143, 161, 203, 234 | →3)-Glc*p*-(1→ |
| | 2,3,6-$Me_3$ | 10.0 | 26.0 | 43, 45, 118, 131, 162, 173, 203, 233, 277 | →4)-Glc*p*-(1→ |
| | 2,6-$Me_2$ | 3.0 | — | 43, 45, 118, 139, 145, 234, 305 | →3,4)-Glc*p*-(1→ |
| | 2,3-$Me_2$ | 10.0 | 20.5 | 43, 118, 129, 162, 233, 261, 305 | →4,6)-Glc*p*-(1→ |
| | 2-Me | — | 2.0 | 43, 118, 173, 261, 301, 333 | →3,4,6)-Glc*p*-(1→ |
| | — | 2.4 | 4.1 | 145, 146, 217, 218, 289, 290 | →2,3,4,6)-Glc*p*-(1→ |

makeup (see Table 5). In that, the main chain was found to be composed of both 1,4- (presence of 2,3,6-$Me_3$-Glc*p*) and 1,3-linked (presence of 2,4,6-$Me_3$-Glc*p*) glucosyl residues, which were further involved in extensive branching. The latter was contributed by multiplely branched glucose (O-3 and O-6 disubstitution as indicated by 2-Me-Glc and O-2, O-4/O-6 trisubstitution as shown by free glucose) moieties. All the arabinose and a portion of xylose and glucose were involved at the non-reducing terminal ends. Unlike Fr. IV, the degree of branching in Fr. V was much more extensive. The latter, may be due to any under-methylation was ruled out by the fact that the polysaccharide was completely soluble in DMSO/dimsyl anion and the resulting permethylated product did not show any –OH absorption at around 3300 $cm^{-1}$ in the IR spectrum (data not shown). FT-IR spectra of the purified polysaccharide fractions showed absorbances characteristic of neutral polysaccharides.[35] The absorbance at 890 $cm^{-1}$ was indicative of β-configuration, whereas that at 1047 $cm^{-1}$ was attributed to arabinan side chain.

In conclusion, the results showed evidence of compositional and structural modifications of both pectic and hemicellulosic polymers during mango fruit ripening. Extensive modification of tightly bound hemicelluloses, specifically the xyloglucan may represent one of the major cell wall polysaccharides contributing for mango fruit ripening phenomenon.

## Acknowledgements

H.M.Y. thanks Council of Scientific and Industrial Research, New Delhi, for a research fellowship.

## References

1. Seymour, G. B.; Colquhoun, I. J.; Dupont, M. S.; Parsely, K. R.; Selvendran, R. R. *Phytochemistry* **1990**, *29*, 725–731.
2. Redgewell, R. J.; Melton, L. D.; Brasch, D. J. *Plant Physiol.* **1992**, *98*, 71–81.
3. Huber, D. J. *J. Am. Soc. Hortic. Sci.* **1983**, *108*, 405–409.
4. Hobson, G. E.; Grierson, D. In *Biochemistry of Fruit Ripening*; Seymour, G. B., Ed.; Chapman and Hall: London, 1993, pp 405–442.
5. Smith, C. J. S.; Watson, C. F.; Ray, J.; Bird, C. R.; Morris, P. C.; Schuch, W.; Grierson, D. *Nature* **1988**, *334*, 724–726.
6. Giovannoni, J. J.; Dellapenne, D.; Bennett, A. B.; Fischer, R. L. *Plant Cell* **1989**, *1*, 53–63.
7. Schuch, R.; Justiniano, E.; Schulz, M.; Datz, S.; Dittner, P. F.; Giese, J. P.; Krause, H. F.; Schone, H.; Vane, R.; Shafroth, S. *Physiol. Rev. A* **1991**, *43*, 5180–5183.
8. Sakurai, N.; Nevins, D. J. *Physiol. Plant* **1993**, *89*, 681–686.
9. Maclachlan, G.; Brady, C. *Plant Physiol.* **1994**, *105*, 965–974.
10. Bhagyalakshmi, N.; Prabha, T. N.; Yashoda, H. M.; Prasanna, V.; Jagadeesh, B. H.; Tharanathan, R. N. *Acta Hortic.* **2002**, *575*, 717–724.
11. Yashoda, H. M.; Prabha, T. N.; Tharanathan, R. N. *J. Sci. Food Agric.*, communicated.
12. Dubois, M.; Gilles, K. A.; Hamilton, J. K.; Rebers, P. A.; Smith, F. *Anal. Chem.* **1956**, *28*, 350–356.
13. Blumenkrantz, N.; Asboe-Hansen, G. *Anal. Biochem.* **1973**, *54*, 484–489.
14. Sawardekar, J. S.; Sloneker, J. H.; Jeanes, A. *Anal. Chem.* **1965**, *37*, 1602–1604.
15. Taylor, R. L.; Conrad, H. E. *Biochemistry* **1972**, *11*, 1383–1388.
16. Hakomori, S. *J. Biochem. (Tokyo)* **1964**, *55*, 205–208.
17. Cutillas-Iturralde, A.; Zarra, I.; Lorences, E. P. *Physiol. Plantarum* **1993**, *89*, 369–375.
18. Brinson, K.; Dey, P. M.; John, M. A.; Pridham, J. B. *Phytochemistry* **1988**, *27*, 719–723.
19. Mitcham, E. J.; McDonald, R. E. *J. Am. Soc. Hortic. Sci.* **1992**, *117*, 919–924.
20. Missang, C. E.; Renard, C. M. G. C.; Baron, A.; Drilleau, J. F. *J. Sci. Food Agric.* **2001**, *81*, 773–780.
21. Gross, K. C.; Wallner, S. J. *Plant Physiol.* **1979**, *63*, 117–120.
22. Hegde, S.; Maness, N. O. *J. Am. Soc. Hortic. Sci.* **1998**, *123*, 445–456.
23. Oesterveld, A.; Beldman, G.; Schols, H. A.; Voragen, A. G. J. *Carbohydr. Res.* **2000**, *328*, 185–197.
24. Strasser, G. R.; Amado, R. *Carbohydr. Polym.* **2002**, *48*, 263–269.
25. Muda, P.; Seymour, G. B.; Errington, N.; Tucker, G. A. *Carbohydr. Polym.* **1995**, *26*, 255–260.
26. Roe, B.; Bruemmer, J. H. *J. Food Sci.* **1981**, *46*, 186–190.
27. Pilnik, W.; Voragen, A. G. J. In *The Biochemistry of Fruits and Their Products*; Hulme, A. C., Ed.; Academic: London, 1970; Vol. 1, pp 53–87.
28. Kacurakova, M.; Capek, P.; Sasinkova, V.; Wellner, N.; Ebringerova, A. *Carbohydr. Polym.* **2000**, *43*, 195–203.
29. Mathlouthi, M.; Koenig, J. L. *Adv. Carbohydr. Chem. Biochem.* **1986**, *44*, 7–89.
30. Davis, E. A.; Derouet, C.; Du Penhoat, C. H. *Carbohydr. Res.* **1990**, *197*, 205–215.
31. Keenan, M. H. J.; Belton, P. S.; Matthew, J. A.; Howson, S. J. *Carbohydr. Res.* **1985**, *138*, 168–170.
32. Newman, R. H.; Redgwell, R. J. *Carbohydr. Polym.* **2002**, *49*, 121–129.
33. Pressey, R.; Himmelsbach, D. S. *Carbohydr. Res.* **1984**, *127*, 356–359.
34. Rose, J. K. C.; Hadfield, K. A.; Labavitch, J. M.; Bennett, A. B. *Plant Physiol.* **1998**, *117*, 345–361.
35. Coimbra, M. A.; Barros, A.; Barros, M.; Rutledge, D. N.; Delgadillo, I. *Carbohydr. Polym.* **1998**, *37*, 241–248.